

# Improved Gauge Actions on Anisotropic Lattices I

## Study of Fundamental Parameters in the Weak Coupling Limit

S.Sakai

Faculty of Education, Yamagata University,  
Yamagata, 990-8560, Japan

T.Saito

Faculty of Science, Hiroshima University,  
Higashi-Hiroshima, 739-8526, Japan

A.Nakamura

Research Institute of Information Sciences and Education,  
Hiroshima University, Higashi-Hiroshima, 739-8521, Japan

### Abstract

On anisotropic lattices with the anisotropy  $\xi = a_\sigma/a_\tau$  the following basic parameters are calculated by perturbative method: (1) the renormalization of the gauge coupling in spatial and temporal directions,  $g_\sigma$  and  $g_\tau$ , (2) the  $\Lambda$  parameter, (3) the ratio of the renormalized and bare anisotropy  $\eta = \xi/\xi_B$  and (4) the derivatives of the coupling constants with respect to  $\xi$ ,  $\partial g_\sigma^{-2}/\partial\xi$  and  $\partial g_\tau^{-2}/\partial\xi$ . We employ the improved gauge actions which consist of plaquette and six-link rectangular loops,  $c_0 P(1 \times 1)_{\mu\nu} + c_1 P(1 \times 2)_{\mu\nu}$ . This class of actions covers Symanzik, Iwasaki and DBW2 actions. The ratio  $\eta$  shows an impressive behavior as a function of  $c_1$ , i.e.,  $\eta > 1$  for the standard Wilson and Symanzik actions, while  $\eta < 1$  for Iwasaki and DBW2 actions. This is confirmed non-perturbatively by numerical simulations in weak coupling regions. The derivatives  $\partial g_\tau^{-2}/\partial\xi$  and  $\partial g_\sigma^{-2}/\partial\xi$  also change sign as  $-c_1$  increases. For Iwasaki and DBW2 actions they become opposite sign to those for standard and Symanzik actions. However, their sum is independent of the type of actions due to Karsch's sum rule.

# 1 Introduction

Anisotropic lattices allow us to carry out numerical simulations with the fine temporal resolution while keeping the spatial lattice spacing coarse, i.e.  $a_\tau < a_\sigma$ , where  $a_\tau$  and  $a_\sigma$  are lattice spacing in the temporal and spatial directions, respectively. This is especially important for QCD Monte Carlo simulation at finite temperature and heavy particle spectroscopy. There have been many such calculations like glue thermodynamics[1], hadron masses at the finite temperature[2], glueballs[3] and heavy quark spectra[4]. The anisotropic lattice may become an important tool for the calculation of the transport coefficients of the quark gluon plasma[5, 6] and for the determination of spectral functions at finite temperature[7, 8]. In numerical simulations on the anisotropic lattice we need the information upon the renormalization of anisotropy which is given by  $\eta = \xi/\xi_B$  where  $\xi$  is the renormalized anisotropy,  $a_\sigma/a_\tau$ , and  $\xi_B$  is the bare one. Karsch has first studied anisotropic lattices perturbatively with the standard plaquette action and obtained  $\eta$  together with anisotropy coefficients which are defined by the derivatives of the spatial and temporal gauge couplings with respect to  $\xi$ , i.e.,  $\partial g_\sigma^{-2}/\partial\xi$  and  $\partial g_\tau^{-2}/\partial\xi$ , and the QCD  $\Lambda$  parameter [9]. In Ref.[10]  $\eta$  was determined non-perturbatively by analyzing Wilson loops in numerical simulations.

Anisotropic lattices play an essential role in the analysis of thermodynamics of QCD. To get the thermodynamics quantities like the internal energy and the pressure from numerical simulations, one needs to know the anisotropy coefficients.

On the anisotropic lattice, we can change the temperature by changing not only  $N_\tau$  but also  $a_\tau$ . This allows us to adjust the temperature continuously with fixed spatial volume.

Recently it has been recognized that improved actions are effective to get reliable results from lattice QCD simulations on the relatively coarse lattice; lattice artifacts due to the discretization are expected to be much less. Therefore, it is important to employ improved actions in the anisotropic lattice calculations, since the lattice is rather coarse in spatial direction in current numerical simulations. García Pérez and van Baal pursued first this direction, i.e., they have determined the one-loop correction to the anisotropy for the square Symanzik improved action[11].

In this article we study the improved actions which consist of plaquette and six-link rectangular loops,

$$S \propto \sum [c_0 P(1 \times 1)_{\mu\nu} + c_1 P(1 \times 2)_{\mu\nu}], \quad (1)$$

where  $c_0$  and  $c_1$  satisfy the relation  $c_0 + 8c_1 = 1$ . This class of actions covers tree level Symanzik action without the tadpole improvement ( $c_1 = -\frac{1}{12}$ ) [12, 13], Iwasaki action ( $c_1 = -0.331$ ) [14] and DBW2 action ( $c_1 = -1.4088$ ) [15]. They are most widely used in simulations of recent days. For the class of actions which consists of planar loops the anisotropic lattice can be formulated in the same way as for the standard plaquette action. This may not be the case for improved actions which include non-planar loops in three or four dimensions.

In the following, we will calculate the  $\Lambda$  parameter,  $\eta = \xi/\xi_B$  and the anisotropy coefficients, in weak coupling regions mainly by perturbative calculations.

In sect. 2 we briefly review the formulation of the anisotropic lattice with the improved actions and summarize formulae which will be used in this paper. In sect. 3, we outline the background field method and discuss the removal of the infrared divergence. In sect. 4 we present results of the perturbative calculations. The  $c_1$  dependence of  $\eta$  and anisotropy coefficients are studied in detail. Since the behavior of  $\eta$  is very important for practical use, we will study it by the numerical simulations in sect. 5. Section 6 is devoted to concluding remarks.

## 2 Anisotropic lattice with improved gauge actions

In case of improved actions that consist of plaquette and rectangular loops, the anisotropic lattice may be formulated in the same way as for the standard plaquette action [9]. The action takes the form

$$S_g = \beta_\sigma \sum_x \sum_{i>j} P_{ij} + \beta_\tau \sum_x \sum_{i \neq 4} P_{4i}, \quad (2)$$

where  $P_{\mu\nu}$  are plaquette and six-link rectangular loop operators in  $\mu$ - $\nu$  plane,

$$P_{\mu\nu} = c_0 P(1 \times 1)_{\mu\nu} + c_1 P(1 \times 2)_{\mu\nu}, \quad (3)$$

which are constructed of the link variable  $U_{n,\mu}$  and

$$\beta_\sigma = \frac{2N_c}{g_\sigma^2(a, \xi)} \xi^{-1}, \quad \beta_\tau = \frac{2N_c}{g_\tau^2(a, \xi)} \xi. \quad (4)$$

Here  $g_\sigma$  and  $g_\tau$  are the coupling constants in the spatial and temporal directions, respectively. The action can be also written with the bare anisotropy

parameter  $\xi_B$  as

$$S_g = \beta_\xi \left( \frac{1}{\xi_B} \sum_x \sum_{i>j} P_{ij} + \xi_B \sum_x \sum_{i\neq 4} P_{4i} \right), \quad (5)$$

where  $\beta_\xi = 2N_c/g_\xi^2 = \sqrt{\beta_\sigma\beta_\tau}$  and  $\xi/\xi_B = \sqrt{g_\tau^2/g_\sigma^2}$ .

The weak coupling limit of the anisotropic lattice is fully discussed in Ref.[9]. Therefore, we will summarize only equations which are necessary in the following studies.

In the continuum limit  $a_\sigma \rightarrow 0$  ( $g \rightarrow 0$ ), the lattice spacing and the coupling  $g_\xi$  are related with each other by the scale parameter  $\Lambda$  through the renormalization group relation,

$$a_\sigma \Lambda(\xi) = (b_0 g_\xi^2)^{-b_1/(2b_0^2)} \exp\{-1/(2b_0 g_\xi^2)\}, \quad (6)$$

where  $b_0$  and  $b_1$  are the universal first two coefficients of  $\beta$ -function,

$$b_0 = \frac{11N_c}{48\pi^2}, \quad b_1 = \frac{34}{3} \left( \frac{N_c}{16\pi^2} \right)^2. \quad (7)$$

We calculate the effective action using the background field method [19] up to one-loop order,

$$\begin{aligned} S_{eff} &= \frac{1}{4} \left( \frac{1}{g_\sigma^2(\xi)} - C_\sigma(\xi) + O(g^2) \right) \sum_{i,j} F_{ij}^2 a_\sigma^3 a_\tau \\ &+ \frac{1}{4} \left( \frac{1}{g_\tau^2(\xi)} - C_\tau(\xi) + O(g^2) \right) \sum_{i\neq 4} (F_{i4}^2 + F_{4i}^2) a_\sigma^3 a_\tau. \end{aligned} \quad (8)$$

Effective actions with different value of the anisotropy parameter  $\xi$  correspond to different regularization scheme, but they should have the same continuum limit and we require  $\Delta S_{eff} = S_{eff}^{\xi\neq 1} - S_{eff}^{\xi=1} = 0$ . Then the relations are obtained,

$$\frac{1}{g_\sigma^2(\xi)} = \frac{1}{g_\sigma^2(1)} + (C_\sigma(\xi) - C_\sigma(1)) + O(g^2), \quad (9)$$

$$\frac{1}{g_\tau^2(\xi)} = \frac{1}{g_\tau^2(1)} + (C_\tau(\xi) - C_\tau(1)) + O(g^2). \quad (10)$$

In the following, the deviation of the one-loop quantum correction from the isotropic case is often employed and written as  $\Delta C_\sigma(\xi) = C_\sigma(\xi) - C_\sigma(1)$ ,  $\Delta C_\tau(\xi) = C_\tau(\xi) - C_\tau(1)$ .

Perturbatively, all fundamental parameters on the anisotropic lattice are given in terms of  $C_\sigma(\xi)$  and  $C_\tau(\xi)$ . The  $\Lambda$  parameter on the anisotropic lattice is given by

$$\frac{\Lambda(\xi)}{\Lambda(1)} = \exp \left\{ -\frac{\Delta C_\sigma(\xi) + \Delta C_\tau(\xi)}{4b_0} \right\}. \quad (11)$$

The quantum correction for the anisotropy parameter  $\eta = \xi/\xi_B$  is written as

$$\eta(\xi, \beta) \equiv \frac{\xi}{\xi_B} = \left( \frac{g_\tau^2}{g_\sigma^2} \right)^{\frac{1}{2}} = 1 + \frac{N_c}{\beta} \eta_1(\xi) + O(\beta^{-2}), \quad (12)$$

$$\eta_1(\xi) = C_\sigma(\xi) - C_\tau(\xi), \quad (13)$$

where  $\Delta C_\sigma(\xi) = 2N_c/g_\sigma^2$  and  $\Delta C_\tau(\xi) = 2N_c/g_\tau^2$  are given by the derivative of the  $C_\sigma(\xi)$  and  $C_\tau(\xi)$  with respect to  $\xi$ ,

$$\frac{\partial g_\sigma^{-2}(\xi)}{\partial \xi} = \frac{\partial C_\sigma(\xi)}{\partial \xi}, \quad \frac{\partial g_\tau^{-2}(\xi)}{\partial \xi} = \frac{\partial C_\tau(\xi)}{\partial \xi}. \quad (14)$$

They play an important role in QCD thermodynamics [9, 10, 16, 17] as will be discussed in section 4.3.

### 3 Perturbative calculation of $C_\sigma$ and $C_\tau$

#### 3.1 Background field method

We calculate  $C_\sigma(\xi)$  and  $C_\tau(\xi)$  in one-loop order, by applying the background field method. The background field method on the lattice is well known [18, 19] and therefore here we will only outline the method of the calculation and stress the points related to the anisotropic lattice. The gauge field is decomposed into a quantum field  $\alpha_\mu$  and a background one  $B_\mu$  which satisfies the classical equation of motion,

$$U_{n,\mu} = e^{ig_\mu a_\mu \alpha_\mu(n)} U_{n,\mu}^{(0)}, \quad U_{n,\mu}^{(0)} = e^{ia_\mu B_\mu(n)}. \quad (15)$$

A gauge fixing term is introduced as,

$$S_{g.f.} = -a_\sigma^3 a_\tau \sum_n \text{Tr} \left( \sum_\mu \overline{D}_\mu^{(0)} \alpha_\mu(n) \right)^2. \quad (16)$$

Here

$$\begin{aligned} D_\mu^{(0)} \alpha_\kappa &= \frac{1}{a_\mu} (U_{n,\mu}^{(0)} \alpha_\kappa(n + \mu) U_{n,\mu}^{(0)\dagger} - \alpha_\kappa(n)), \\ \overline{D}_\mu^{(0)} \alpha_\kappa &= \frac{1}{a_\mu} (U_{n,-\mu}^{(0)} \alpha_\kappa(n - \mu) U_{n,-\mu}^{(0)\dagger} - \alpha_\kappa(n)). \end{aligned} \quad (17)$$

The Faddeev-Popov term resulting from the gauge fixing is

$$S_{F.P.} = -2a_\sigma^3 a_\tau \sum_n \sum_\mu \text{Tr}[(D_\mu^{(0)}\phi(n))^\dagger (D_\mu^{(0)}\phi(n))]. \quad (18)$$

The total action becomes

$$S_{tot}(\alpha_\mu, \phi, B_\mu) = S_g(\alpha_\mu, B_\mu) + S_{g.f.}(\alpha_\mu, B_\mu) + S_{F.P.}(\phi, B_\mu), \quad (19)$$

where  $S_g$  is the gauge action constructed from plaquette and six-link rectangle loops. It is invariant under the following gauge transformation,

$$\begin{cases} U_{n,\mu}^{(0)} & \rightarrow V(n)U_{n,\mu}^{(0)}V^\dagger(n+\mu) \\ \alpha_\mu(n) & \rightarrow V(n)\alpha_\mu(n)V^\dagger(n) \\ \phi(n) & \rightarrow V(n)\phi(n)V^\dagger(n), \end{cases} \quad (20)$$

$$\begin{cases} D_\mu\phi(n) & \rightarrow V(n)D_\mu\phi(n)V^\dagger(n) \\ \bar{D}_\mu\phi(n) & \rightarrow V(n)\bar{D}_\mu\phi(n)V^\dagger(n), \end{cases} \quad (21)$$

where  $V$  is an element of  $SU(N_c)$ . For the calculation of the effective action in one-loop order we expand the total action up to second order in  $\alpha_\mu$  and  $B_\mu$ , which we denote as  $S_{tot}^{(2)}$ . With the help of Campbell-Hausdorff's formula and a relation  $V \exp(i\alpha) = \exp(iV\alpha V^{-1})V$ , we split the total action into a classical action and a bilinear term of  $\alpha_\mu$  and  $\phi$ ,

$$S_{tot} = S(B_\mu) + S_{tot}^{(2)}(\alpha_\mu, \phi, B_\mu). \quad (22)$$

The term linear in  $B_\mu$  is missing because of the equation of motion for the background field.

Thanks to the gauge invariance of the background field, it is sufficient to calculate the coefficients of  $p_\mu p_\nu B_\mu B_\nu$  to obtain the effective action. For the calculation of this term, we have applied the method explained in the appendix of Ref.[20], which makes the calculation much simpler.

It is convenient to separate the action  $S_{tot}^{(2)}$  into several parts, i.e.,  $S_{tot}^{(2)} = S_0 + S'_0 + \dots + S'_6 + S_{F.P.}$ .  $S_0, S'_0, \dots$  and  $S'_6$  are symbolically expressed as

follows[20]

$$\left\{ \begin{array}{l} S_0 : f^2 \\ S'_0 : (\Delta\alpha)^2 \\ S_1 : f[B, \alpha] \\ S'_1 : \Delta\alpha[B, \alpha] \\ S_2 : [\alpha, \alpha]W \\ S_3 : [B, \alpha][B, \alpha] \\ S_4 : f[B, [B, \alpha]] \\ S_5 : [[B, \alpha], \alpha]W \\ S_6 : f^2W^2 \\ S'_6 : \alpha W[\alpha, W], \end{array} \right. \quad (23)$$

where  $B$  and  $\alpha$  represent  $B_\mu$  and  $\alpha_\mu$ , respectively and  $W$  and  $f$  are the field strength tensors of background and quantum fields, respectively.  $\Delta$  is a lattice derivative when we set  $U^{(0)} = 1$  in Eq.(17).  $S_0$  and  $S'_0$  are the free part of the action, which defines gluon propagators.  $S_1$ ,  $S'_1$  and  $S_2$  terms correspond to three-point diagram from which we construct the one-loop self-energy.  $S_3$  to  $S'_6$  contribute to the tadpole self-energy. Here  $S'_0$  and  $S'_1$  result from gauge fixing terms. The Faddeev-Popov term is the same as the previous calculations except that the anisotropy parameter  $\xi$  is included [18, 19].

### 3.2 Effects of anisotropy parameters

By the integration over the quantum fields, we obtain the effective action in one-loop order. We carry out the integration in the momentum space. Fourier transform of the gauge and Faddeev-Popov fields are defined as

$$a_\mu \alpha_\mu(n + 1/2) = \int_{-\pi}^{\pi} a_\mu \alpha_\mu(ka) \exp(i(n + 1/2)ka) \prod_{\nu} \frac{d(k_\nu a_\nu)}{2\pi}, \quad (24)$$

$$a_\sigma \phi(n) = \int_{-\pi}^{\pi} a_\sigma \phi(ka) \exp(ink a) \prod_{\nu} \frac{d(k_\nu a_\nu)}{2\pi}. \quad (25)$$

We also define Fourier transformation of the classical field in a similar manner.

By this Fourier transformation, the anisotropy parameters are factorized in the action  $S_{tot}^{(2)}$ .

$$S_{tot, \mu\nu}^{(2)}(\xi) = X_{\mu\nu} S_{tot, \mu\nu}^{(2)}(1) \quad (26)$$

$S_{tot,\mu\nu}^{(2)}(1)$  are already given by Iwasaki and Sakai[20] on the isotropic lattice and  $X_{\mu\nu}$  are defined as

$$X_{\mu\nu} = \begin{bmatrix} \frac{1}{\xi}, \frac{1}{\xi}, \frac{1}{\xi}, \xi \\ \frac{1}{\xi}, \frac{1}{\xi}, \frac{1}{\xi}, \xi \\ \frac{1}{\xi}, \frac{1}{\xi}, \frac{1}{\xi}, \xi \\ \xi, \xi, \xi, \xi^3 \end{bmatrix}. \quad (27)$$

In this way the perturbative calculation of the anisotropic lattice becomes very systematic and transparent.

For example the free part of the anisotropic improved action  $S_0$  is given by

$$S_0 = -\frac{1}{2} \int_k \sum_{\mu,\nu} \alpha_\mu(ka) G_{\mu\nu} \alpha_\nu(-ka), \quad (28)$$

$$\begin{cases} G_{ii} &= \frac{1}{\xi} \{q_{i4} \hat{k}_i^2 + \hat{k}_i^2\} + \xi q_{i4} \hat{k}_4^2 \\ G_{44} &= \xi q_{44} \hat{k}_4^2 + \xi^3 \hat{k}_4^2 \\ G_{ij} &= \frac{1}{\xi} \{1 - q_{ij}\} \hat{k}_i \hat{k}_j \\ G_{4j} &= \xi \{1 - q_{4j}\} \hat{k}_4 \hat{k}_j \\ G_{j4} &= G_{4j}, \end{cases} \quad (29)$$

$$\begin{cases} \hat{k}_\mu &= 2 \sin \frac{1}{2} k_\mu a \\ q_{\mu\nu} &= 1 - c_1 (\hat{k}_\mu^2 + \hat{k}_\nu^2) \quad (\mu \neq \nu) \\ q_{\nu\nu} &= 0, \end{cases} \quad (30)$$

where the  $\xi^3$  term in  $G_{44}$  results from the gauge fixing term and  $\int_k$  stands for  $\prod_{\mu=1}^4 \int_{-\pi}^{\pi} dk_\mu a_\mu / 2\pi$ . Note that off-diagonal elements of  $G_{\mu\nu}$  vanish for the Wilson action.

Propagators  $D_{\mu\nu}$  are defined by

$$\langle \alpha_\mu^i(ka) \alpha_\nu^j(k'a) \rangle = \delta_{ij} (2\pi)^4 \delta^{(4)}(ka + k'a) D_{\mu\nu}(ka), \quad (31)$$

and they are obtained by solving the equations,

$$G_{\mu\rho} D_{\rho\nu} = \delta_{\mu\nu}. \quad (32)$$

The Faddeev-Popov propagator is given by

$$D_{F.P.}(ka) = \frac{\xi}{\hat{k}_i^2 + \xi^2 \hat{k}_4^2}. \quad (33)$$



The explicit forms of the  $S_1$  to  $S'_6$  terms in Eq.(23) are obtained by setting  $c_2 = c_3 = 0$  in formulae of Ref.[20] and by introducing the anisotropy factors as shown in Eqs. (26) and (27).

The effective action is obtained by integrating  $S_{tot}^{(2)}(\alpha_\mu, \phi, B_\mu)$  over  $a_\mu\alpha_\mu$  and Faddeev-Popov fields  $a_\sigma\phi$ ,

$$e^{-S(a_\mu B_\mu)} \int \mathcal{D}(a_\mu\alpha_\mu)\mathcal{D}(a_\sigma\phi)e^{-S_{tot}^{(2)}(a_\mu\alpha_\mu, a_\sigma\phi, a_\mu B_\mu)} = e^{-S_{eff}(a_\mu B_\mu)}. \quad (34)$$

Then  $C_\sigma(\xi)$  and  $C_\tau(\xi)$  in Eq.(8) are obtained as coefficients of  $F_{ij}^2$  and  $F_{i4}^2$  in  $S_{eff.}$ , respectively.

### 3.3 Infrared divergence

We will discuss here a subtle point concerning the cancellation of the infrared divergence. The contributions for  $C_\sigma$  and  $C_\tau$  from the self-energy type diagram of the term  $\langle (S_1 + S_2)^2 \rangle$  have the infrared divergence. However in the difference given by Eqs. (9) and (10) they are canceled. But numerically the calculation of the divergent integral is very delicate problem. In the numerical evaluation, we discretize the momentum integration  $\int d^4k$ , and the divergence comes from the segment including  $k = 0$ . We should not take the difference of integration with different  $\xi$  directly, because their measures of segment are different for isotropic and anisotropic lattices. We use the following method for the calculation of the Eqs. (9) and (10),

$$\begin{aligned} C_\sigma^{Imp.}(\xi) - C_\sigma^{Imp.}(1) &= (C_\sigma^{Imp.}(\xi) - C_\sigma^{Stand.}(\xi)) \\ &+ (C_\sigma^{Stand.}(\xi) - C_\sigma^{Stand.}(1)) \\ &+ (C_\sigma^{Stand.}(1) - C_\sigma^{Imp.}(1)). \end{aligned} \quad (35)$$

where  $C_\sigma^{Imp.}$  and  $C_\sigma^{Stand.}$  are the coefficients with improved and standard actions, respectively.

In the first term of r.h.s of Eq.(35),  $C_\sigma^{Imp.}(\xi)$  and  $C_\sigma^{Stand.}(\xi)$  have the same infrared divergence and they are canceled exactly by each other. The second term of Eq.(35) can be calculated by the analytic integration of the 4th component of the loop momentum[9]. The results do not include the infrared divergence and the numerical integration is stable. The divergence in the last term has been already calculated in Ref.[20]. We have checked that our calculations for the second and the third terms of Eq.(35) coincide with those for Wilson and Symanzik case respectively given in Ref.[9] and

Ref.[20]<sup>1</sup>.

In this way the difference  $C_\sigma^{Imp.}(\xi) - C_\sigma^{Imp.}(1)$  is calculated in numerically stable manner. Similar calculation has been done for  $C_\tau^{Imp.}(\xi) - C_\tau^{Imp.}(1)$ .

## 4 Results of one-loop calculation

Values of  $C_\sigma(\xi) - C_\sigma(1)$  and  $C_\tau(\xi) - C_\tau(1)$  are given in Table 1 for Symanzik, Iwasaki and DBW2.  $\xi$  is varied from 1 to 6, since these anisotropy parameters are often used in Monte Carlo simulations on anisotropic lattices.

	$\xi$	Symanzik action		Iwasaki action		DBW2 action	
		$\Delta C_\sigma$	$\Delta C_\tau$	$\Delta C_\sigma$	$\Delta C_\tau$	$\Delta C_\sigma$	$\Delta C_\tau$
SU(2)	1.0	0.00000	0.00000	0.00000	0.00000	0.00000	0.00000
	1.1	0.00541	-0.00092	-0.00201	0.00614	-0.01124	0.01464
	1.5	0.02072	-0.00173	-0.00908	0.02327	-0.04875	0.05150
	2.0	0.03180	-0.00085	-0.01564	0.03612	-0.08400	0.07510
	3.0	0.04304	0.00103	-0.02406	0.05016	-0.13384	0.09537
	4.0	0.04862	0.00159	-0.02934	0.05613	-0.16932	0.09766
	5.0	0.05168	0.00059	-0.03340	0.05692	-0.19695	0.09055
	6.0	0.05314	-0.00162	-0.03725	0.05444	-0.21970	0.08000
SU(3)	1.0	0.00000	0.00000	0.00000	0.00000	0.00000	0.00000
	1.1	0.00930	-0.00253	-0.00427	0.01045	-0.02087	0.02584
	1.5	0.03602	-0.00701	-0.01852	0.03967	-0.08983	0.09206
	2.0	0.05571	-0.00829	-0.03119	0.06184	-0.15389	0.13609
	3.0	0.07596	-0.00856	-0.04693	0.08679	-0.24348	0.17729
	4.0	0.08614	-0.00951	-0.05644	0.09843	-0.30658	0.18776
	5.0	0.09182	-0.01216	-0.06350	0.10163	-0.35533	0.18221
	6.0	0.09462	-0.01625	-0.07012	0.09953	-0.39532	0.17034

Table 1:  $C_\sigma$  and  $C_\tau$  for Symanzik, Iwasaki and DBW2 actions. Here  $\Delta C_\sigma = C_\sigma(\xi) - C_\sigma(1)$  and  $\Delta C_\tau = C_\tau(\xi) - C_\tau(1)$ .

### 4.1 The $\Lambda$ ratio

When we calculate physical quantities, we must take into account the variation of the scale  $a_\sigma$  due to  $\Lambda(\xi)$ . In weak coupling regions it is given by

<sup>1</sup>Although the values of  $C_\sigma^{Stand.}(\xi) - C_\sigma^{Stand.}(1)$  were not given in Ref.[9], we have calculated them from Table and formulae in Ref.[9]

Eq.(11). The  $\Lambda$  ratio is calculated as a product of three factors,

$$\frac{\Lambda_{Imp.}(\xi)}{\Lambda_{Imp.}(1)} = \frac{\Lambda_{Imp.}(\xi)}{\Lambda_{Stand.}(\xi)} \times \frac{\Lambda_{Stand.}(\xi)}{\Lambda_{Stand.}(1)} \times \frac{\Lambda_{Stand.}(1)}{\Lambda_{Imp.}(1)}. \quad (36)$$

The numerical results are given in the Table 2 for Symanzik, Iwasaki and DBW2 and are shown in Fig. 1.

		$\Lambda_{Imp.}(\xi)/\Lambda_{Imp.}(1)$			$\Lambda_{Imp.}(\xi)/\Lambda_{Imp.}(1)$			
$\xi$		Symanzik	Iwasaki	DBW2				
		Symanzik	Iwasaki	DBW2	Symanzik	Iwasaki	DBW2	
SU(2)	1.0	1.00000	1.00000	1.00000	SU(3)	1.00000	1.00000	1.00000
	1.1	0.97614	0.97803	0.98187		0.97599	0.97809	0.98234
	1.5	0.90282	0.92641	0.98529		0.90111	0.92691	0.99204
	2.0	0.84653	0.89562	1.04907		0.84350	0.89583	1.06597
	3.0	0.78873	0.86890	1.23013		0.78512	0.86670	1.26812
	4.0	0.76309	0.86566	1.47071		0.75955	0.86010	1.53177
	5.0	0.75471	0.88107	1.77320		0.75133	0.87209	1.86138
	6.0	0.75778	0.91159	2.12140		0.75483	0.89981	2.24211

Table 2:  $\Lambda$  parameter ratio for improved actions.

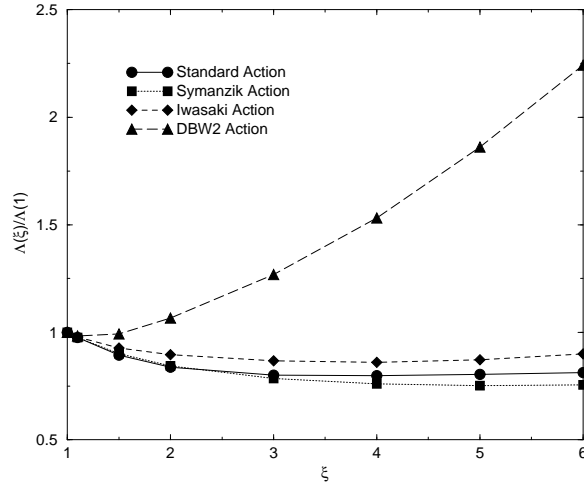


Figure 1: The ratio of  $\Lambda$  parameter for SU(3).

## 4.2 The $\eta$ parameter

The  $\eta$  parameter is given by Eqs. (12) and (13). Because of the gauge invariance we can see  $C_\sigma(1) = C_\tau(1)$  at the isotropic case, and therefore these coefficients do not appear in the definition of  $\eta$ . But to cancel the infrared divergence we calculate Eq.(13) as  $\eta_1(\xi) = (C_\sigma(\xi) - C_\sigma(1)) - (C_\tau(\xi) - C_\tau(1))$ . We plot  $\eta_1$  as a function of  $c_1$  in Fig. 2.

	$\xi$	Symanzik	Iwasaki	DBW2		Symanzik	Iwasaki	DBW2
SU(2)	1.0	0.00000	0.00000	0.00000	SU(3)	0.00000	0.00000	0.00000
	1.1	0.00633	-0.00816	-0.02588		0.01183	-0.01472	-0.04671
	1.5	0.02246	-0.03235	-0.10025		0.04303	-0.05820	-0.18190
	2.0	0.03266	-0.05177	-0.15911		0.06400	-0.09304	-0.28998
	3.0	0.04201	-0.07423	-0.22921		0.08452	-0.13372	-0.42077
	4.0	0.04702	-0.08548	-0.26698		0.09565	-0.15487	-0.49434
	5.0	0.05109	-0.09032	-0.28751		0.10398	-0.16513	-0.53755
	6.0	0.05476	-0.09170	-0.29971		0.11088	-0.16966	-0.56567

Table 3: The  $\eta_1$  for improved actions.

The parameter  $\eta_1$  changes sign around  $c_1 = -0.18 \sim -0.19$ . This means that in weak coupling regions, there is no renormalization for the anisotropy parameter  $\xi$  for this action. The interesting point is that the  $\beta$  dependence of the  $\eta$  with Iwasaki and DBW2 actions is opposite to those with standard and Symanzik actions; As  $\beta$  decreases  $\eta$  decreases for Iwasaki and DBW2 action, while it increases for standard and Symanzik actions. This is a new feature and we shall confirm it non-perturbatively in the next section.

## 4.3 Anisotropy coefficients

The anisotropy coefficients, which are the derivatives of spatial and temporal gauge couplings with respect to the anisotropy  $\xi$ , are calculated as,

$$\frac{\partial g_\sigma^{-2}}{\partial \xi} = \frac{\partial}{\partial \xi} (C_\sigma^{Imp.}(\xi) - C_\sigma^{Stand.}(\xi)) + \frac{\partial}{\partial \xi} (C_\sigma^{Stand.}(\xi) - C_\sigma^{Stand.}(1)). \quad (37)$$

In this manner, we are free from the infrared divergence, and the numerical evaluation is stable as in Sect. 3.3.

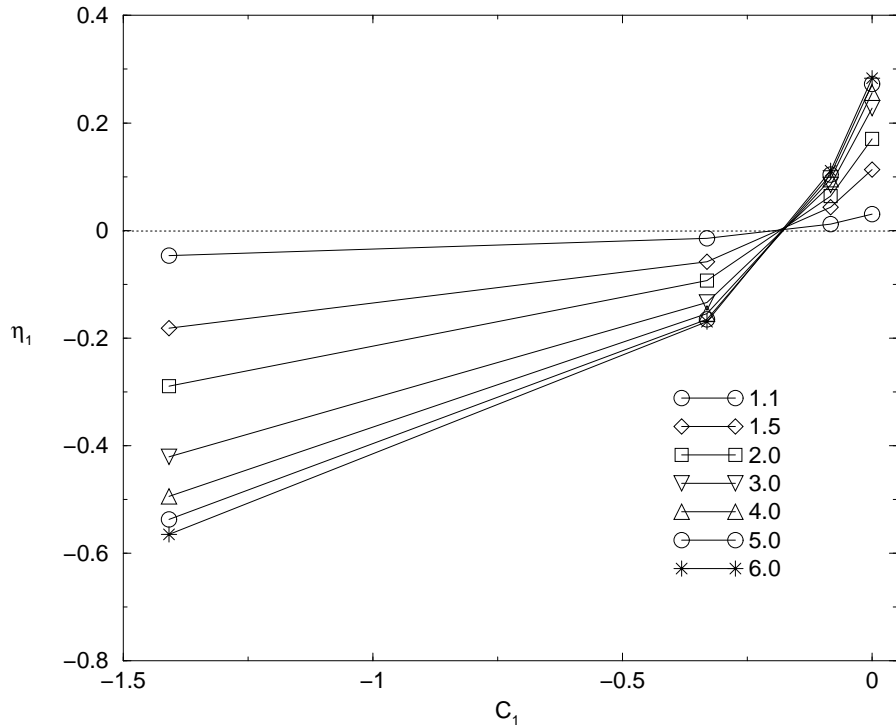


Figure 2: The  $\eta_1$  as a function of  $c_1$  for SU(3).

From the invariance of the string tension on the isotropic and anisotropic lattice, Karsch has derived the following sum rule[9],

$$\frac{\partial g_\sigma^{-2}}{\partial \xi} + \frac{\partial g_\tau^{-2}}{\partial \xi} = \frac{11N_c}{48\pi^2} \quad (\xi = 1, a \rightarrow 0). \quad (38)$$

The same arguments are applied to improved actions. We show results in Table 4 and Fig. 3. This sum rule is satisfied quite well.

An interesting point is that individual terms  $\partial g_\sigma^{-2}/\partial \xi$  and  $\partial g_\tau^{-2}/\partial \xi$  also change sign as  $-c_1$  increases. For Iwasaki and DBW2 actions,  $\partial g_\tau^{-2}/\partial \xi$  becomes positive while it is negative for standard and Symanzik actions. These anisotropy coefficients have a contribution to QCD thermodynamics. For example, Okamoto et al.[22] used our perturbation results to study the energy and pressure with Iwasaki action and had no negative pressure problem, contrary to Wilson action case[23].

## 5 Numerical results in weak coupling regions

In the previous section we have found by the perturbative calculation that the ratio of the renormalized and bare anisotropy,  $\eta$ , becomes less than one for Iwasaki and DBW2 actions.

Since the  $\eta$  is important in QCD simulations on the anisotropic lattice, we will study its behavior further by numerical simulations.

Numerically the  $\eta$  parameter is calculated from the relation [10, 24],

$$\eta = \xi/\xi_B. \quad (39)$$

The anisotropy  $\xi_B$  appears in the action given by Eq.(5) while the renormalized anisotropy  $\xi$  is defined by

$$\xi = a_\sigma/a_\tau. \quad (40)$$

For the probe of the scale in the space and temperature direction, we use the lattice potential in these directions, which is defined by

$$V_{\sigma\tau}(\xi_B, l, t) = \ln\left(\frac{W_{\sigma\tau}(l, t)}{W_{\sigma\tau}(l+1, t)}\right), \quad (41)$$

where  $W_{\sigma\tau}(l, t)$  is the Wilson loop of the size  $l \times t$  in the temporal plane. Similar formula holds for the potential in space direction. We fix  $\xi = 2$ , and calculate the ratio at a few  $\xi_B$  points,

$$R(\xi_B, l, r) = \frac{V_{\sigma\sigma}(\xi_B, l, r)}{V_{\sigma\tau}(\xi_B, l, \xi t)}. \quad (42)$$

Then we search for the point  $R = 1$  by interpolating  $\xi_B$ [10, 24]. In Ref.[25], an extensive study is done for the determination of  $\xi_B$ .

	SU(2)		SU(3)	
	$\partial g_\sigma^{-2}/\partial\xi _{\xi=1}$	$\partial g_\tau^{-2}/\partial\xi _{\xi=1}$	$\partial g_\sigma^{-2}/\partial\xi _{\xi=1}$	$\partial g_\tau^{-2}/\partial\xi _{\xi=1}$
Symanzik	0.058406	-0.01196	0.10025	-0.030365
Iwasaki	-0.020569	0.067009	-0.044305	0.113965
DBW2	-0.117103	0.163543	-0.21793	0.287592

Table 4: The anisotropy coefficients for improved actions. The results are checked by estimating the derivative numerically by using the results with  $\xi = 1.05, 1.1$ .

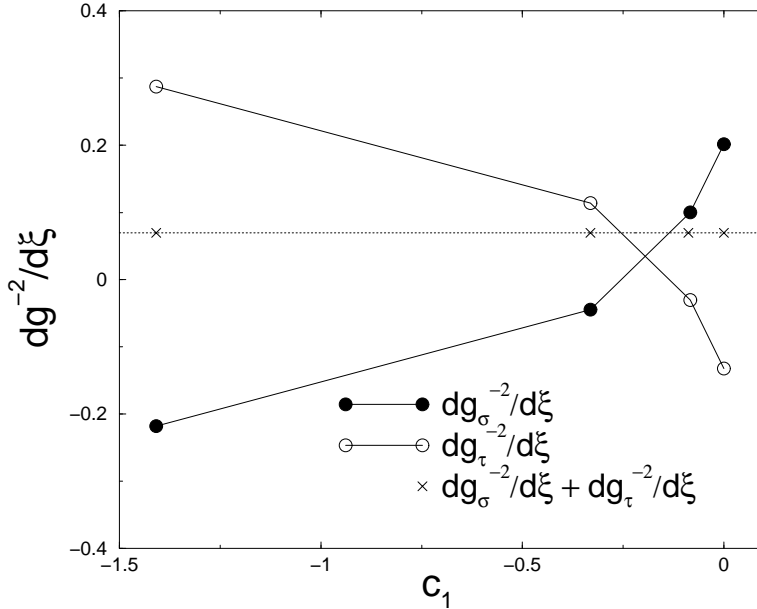


Figure 3: Anisotropy coefficients with the standard and improved actions for SU(3). Dotted line represents the r.h.s of Eq.(38), which is about 0.0697 for SU(3) case. The cross symbol stands for the l.h.s of Eq.(38).

The simulations are done on the  $12^3 \times 24$  lattice. Numerical results with large  $\beta$  region ( $\beta \geq 10$ ) together with perturbative ones are shown in Fig. 4. They agree with each other at large  $\beta$  region. The  $\eta$  parameter decreases as  $\beta$  decreases for Iwasaki and DBW2 while it increases for standard and Symanzik actions.

## 6 Concluding remarks

We have calculated the QCD scale parameter  $\Lambda$ , which is shown in Table 2 and Fig. 1. Ratios  $\Lambda(\xi)/\Lambda(1)$  for standard, Symanzik and Iwasaki actions have very similar behavior; they are slightly less than one, but the behavior of  $\Lambda$  ratio of the DBW2 is quite different from those of other actions. DBW2 action is expected to be very near to the renormalized trajectory[15], and may have a special feature. It may be interesting to study the  $c_1$  dependence of the  $\Lambda$  parameters between Iwasaki and DBW2 actions in more detail.

The  $\eta$  parameters and anisotropy coefficients, the derivatives of the cou-

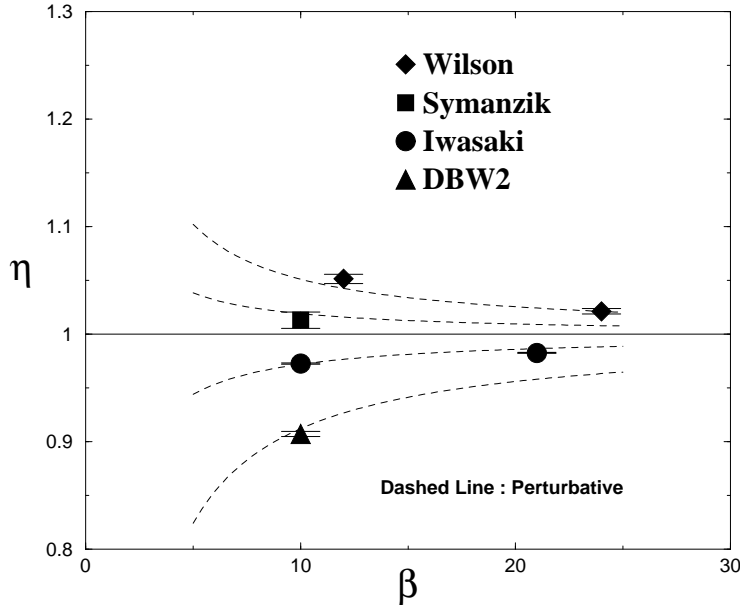


Figure 4: Perturbative and non-perturbative results of  $\eta$  as a function of  $\beta$ . Data for Wilson actions are taken from Ref.[24]

pling constants with respect to the anisotropy parameter  $\xi$  are calculated in one-loop order for improved actions. We have found that the  $\eta_1$  in the Eq.(13) changes sign for  $c_1 \simeq -0.18 \sim -0.19$  as shown in Fig. 2. The  $\eta_1(\xi)$  is positive for the standard plaquette and Symanzik actions while it becomes negative for Iwasaki and DBW2 actions. This behavior is confirmed non-perturbatively by the numerical simulations in weak coupling regions as shown in Fig. 4.

We have also found that the anisotropy coefficients change sign as  $-c_1$  increases. For Iwasaki and DBW2 actions,  $\partial g_\tau^{-2}/\partial \xi$  is positive while for standard and Symanzik actions it is negative. These may be good properties for the thermodynamics using those improved actions[22].

We have found that  $\eta$  obtained by the perturbation calculations is close to one in the region  $c_1 \simeq -0.18 \sim -0.19$  for  $\xi = 1 \sim 6$ <sup>2</sup>. A natural question is whether this is true also at intermediate and strong coupling regions.

<sup>2</sup>The value is slightly shifted from that in Ref.[21]. After lattice'99, we have done an extensive study of the numerical calculation of the loop integral, so that we can safely extrapolate to the continuum integral.



Parts of the results on the  $\eta$  parameter are reported at lattice '99 at Pisa[21]. The study of the lattice spacing  $a$  on the anisotropic lattice in intermediate coupling regions has been started. Detailed results will be reported in the forthcoming paper. Moreover, with these fundamental properties of the improved actions on anisotropic lattices, we are going to start simulations of heavy quark spectroscopy, transport coefficients of quark gluon plasma etc. on these lattices.

### Acknowledgments

We are grateful to R. V. Gvai for the discussion for thermodynamics quantities. This work is supported by the Grant-in-Aide for Scientific Research by Monbusho, Japan (No. 10640272). In this work, QCD Monte Carlo simulations have been done on SX-4 at RCNP, Osaka Univ. and on VPP500 at KEK(High Energy Accelerator Research Organization) and Tsukuba Univ..

### Appendix

In this appendix we show all the data used in Eq.(35). In Table 5 the data of the first term in Eq.(35) are summarized, and in Table 6 we report the data for the standard action. The values of the third terms in Eq.(35) are given by isotropy cases in Table 5.

	$\xi$	Symanzik action		Iwasaki action		DBW2 action	
		$\delta C_\sigma(\xi)$	$\delta C_\tau(\xi)$	$\delta C_\sigma(\xi)$	$\delta C_\tau(\xi)$	$\delta C_\sigma(\xi)$	$\delta C_\tau(\xi)$
SU(2)	1.0	-0.13173	-0.13173	-0.32668	-0.32668	-0.57505	-0.57505
	1.1	-0.13690	-0.12672	-0.33928	-0.31461	-0.59687	-0.55447
	1.5	-0.15149	-0.11355	-0.37625	-0.28349	-0.66429	-0.50362
	2.0	-0.16130	-0.10393	-0.40371	-0.26190	-0.72042	-0.47128
	3.0	-0.16908	-0.09261	-0.43115	-0.23844	-0.78929	-0.44160
	4.0	-0.17135	-0.08643	-0.44427	-0.22685	-0.83262	-0.43368
	5.0	-0.17218	-0.08359	-0.45223	-0.22221	-0.86414	-0.43694
	6.0	-0.17292	-0.08300	-0.45828	-0.22188	-0.88909	-0.44468
SU(3)	1.0	-0.23211	-0.23211	-0.57349	-0.57349	-0.99987	-0.99987
	1.1	-0.24156	-0.22293	-0.59652	-0.55132	-1.03950	-0.96232
	1.5	-0.26836	-0.19832	-0.66429	-0.49302	-1.16198	-0.86701
	2.0	-0.28649	-0.17988	-0.71477	-0.45112	-1.26386	-0.80326
	3.0	-0.30099	-0.15771	-0.76527	-0.40373	-1.38820	-0.73962
	4.0	-0.30524	-0.14509	-0.78921	-0.37852	-1.46573	-0.71558
	5.0	-0.30674	-0.13848	-0.80344	-0.36606	-1.52166	-0.71187
	6.0	-0.30799	-0.13586	-0.81412	-0.36144	-1.56570	-0.71702

Table 5:  $C_\sigma$  and  $C_\tau$  for Symanzik, Iwasaki and DBW2 actions. Here  $\delta C_\sigma(\xi) = C_\sigma^{Imp.}(\xi) - C_\sigma^{Stand.}(\xi)$  and  $\delta C_\tau(\xi) = C_\tau^{Imp.}(\xi) - C_\tau^{Stand.}(\xi)$ .

## References

- [1] T.Hashimoto, A.Nakamura and I.O.Stamatescu, Nucl. Phys. B400 (1993) 267.
- [2] QCD-TARO Collaboration, Ph. de Forcrand et al., hep-lat/9911001.
- [3] C.Morningstar and M.Pearson, Phys. Rev. D56 (1997) 4043.
- [4] T.R. Klassen, Nucl. Phys. B(Proc.Suppl.) 73 (1999) 918.
- [5] F.Karsch and H.W.Wyld, Phys. Rev. D35, 2518.
- [6] A.Nakamura, S.Sakai and K.Amemiya, Nucl. Phys. B(Proc.Suppl.)42 (1996) 432; A.Nakamura, T.Saito and S.Sakai, Nucl. Phys. B(Proc.Suppl.)63 (1998) 424.
- [7] QCD-TARO Collaboration, Ph. de Forcrand et al., Nucl. Phys. B(Proc. Suppl.) 63A-C (1998) 460.
- [8] Y.Nakahara, M.Asakawa and T.Hatsuda, Phys. Rev. D60 091503.

	$\xi$	$\Delta C_\sigma(\xi)$	$\Delta C_\tau(\xi)$		$\Delta C_\sigma(\xi)$	$\Delta C_\tau(\xi)$
SU(2)	1.0	0.00000	0.00000	SU(3)	0.00000	0.00000
	1.1	0.01058	-0.00593		0.01875	-0.01171
	1.5	0.04048	-0.01991		0.07227	-0.04079
	2.0	0.06137	-0.02865		0.11009	-0.06051
	3.0	0.08039	-0.03807		0.14485	-0.08296
	4.0	0.08824	-0.04370		0.15928	-0.09652
	5.0	0.09213	-0.04754		0.16645	-0.10578
	6.0	0.09433	-0.05035		0.17051	-0.11250

Table 6:  $C_\sigma$  and  $C_\tau$  for the standard action.  $\Delta C_\sigma(\xi) = C_\sigma^{Stand.}(\xi) - C_\sigma^{Stand.}(1)$  and  $\Delta C_\tau(\xi) = C_\tau^{Stand.}(\xi) - C_\tau^{Stand.}(1)$ . We have evaluated these data from Table and formulae in Ref.[9].

- [9] F.Karsch, Nucl. Phys. B205[FS5] (1982) 285.
- [10] G.Burgers, F.Karsch, A.Nakamura and I.O.Stamatescu, Nucl. Phys. B304 (1988) 587.
- [11] M. García Pérez and P. van Baal, Phys. Lett. B 392 (1997)163.
- [12] K.Symanzik, Nucl. Phys. B226 (1983) 187.
- [13] M.Lüscher and P. Weisz, Phys. Lett. 158B (1985) 250.
- [14] Y.Iwasaki, Univ. of Tsukuba report UTHEP-118 (1983); Nucl. Phys. B258 (1985) 141.
- [15] QCD-TARO Collaboration, Ph. de Forcrand et al., hep-lat/9911033.
- [16] J.Engels, F.Karsch, H.Satz and I.Montvay, Nucl. Phys. B205[FS5] (1982) 545.
- [17] S.Ejiri, Y.Iwasaki and K.Kanaya, Phys. Rev. D58 (1998) 094505.
- [18] A.Hasenfratz and P.Hasenfratz, Phys. Lett. 93B (1980) 165, A.Hasenfratz and P.Hasenfratz, Nucl. Phys. B193 (1981) 210.
- [19] R.Dashen and D.J.Gross, Phys. Rev. D23 (1981) 2340.
- [20] Y.Iwasaki and S.Sakai, Nucl. Phys. B248 (1984) 441.
- [21] S.Sakai, A.Nakamura and T.Saito, hep-lat/0001004.

- [22] M.Okamoto et al., CP-PACS Collaboration, Phys. Rev. D60 094510.
- [23] B.Svetitsky and F.Fucito, Phys. Lett. 131B (1983) 165.
- [24] T.R. Klassen, Nucl. Phys. B 533 (1998) 557.
- [25] J.Engels, F.Karsch, T.Scheideler, Nucl. Phys. B564(2000)303.